J. of the Chosun Natural Science
Vol. 3, No. 1 (2010) pp. 33 – 37

Biosensor Based on Distributed Bragg Reflector Photonic Crystals for the Detection of Protein A

Daehyuk Jung†

Abstract

The functionalized photonic crystals of porous silicon biosensor was prepared for the application as a label-free biosensor based on distributed Bragg reflector interferometer. Prepared distributed Bragg reflector of porous silicon biosensor displayed sharp reflection in the optical reflective spectra. The mean of construction of molecular architectures on distributed Bragg reflector of porous silicon surfaces was investigated for the step-by-step binding interaction with amines, biotin, avidin, and biotinylated protein A. The subsequent introduction of avidin, and biotinylated protein A resulted in the reflectivity shifted to longer wavelengths, indicative of a change in refractive indices induced by binding of biomolecules.

Key words : Porous silicon, Photonic Structure, Biosensor, Red Shift

1. Introduction

Porous silicon(PSi) obtained by chemical or electrochemical dissolution of crystalline silicon has shown a great quantity of applications and extensive works on this material has been reported both in the scientific and technological areas. The visible photoluminescence at room temperature of this material reported in 1990 by Canham has attracted considerable interest due to the possibility of manufacture an integrated optical device on Si. Porous silicon multilayers, sometimes also called porous silicon superlattices, improve the feasibility of optical components realized from this interesting material : distributed Bragg reflectors(DBR) and Fabry-Perot interferential filters, microcavities with controlled spontaneous emission properties, waveguides, colour-sensitive photodiodes, and resonant cavity light emitting diodes are some of them. By adjusting the electrochemical etching conditions such as alternating current densities, time, and HF concentration, the morphology and porosity of PSi can be easily controlled. DBR PSi exhibits unique optical properties. DBR PSi has been typically prepared by an applying a computer generated pseudo-square current waveform to the etch cell which results two distinct indices and exhibits photonic structure of Bragg filters.

Since the early studies of Ulhir, Tuner, and later Canham, porous silicon has been widely investigated for electronics, optoelectronics, and sensor application.[1] Porous silicon can be prepared by chemical or electrochemical etching processes and consists of nano or microcrystalline morophologies. The diameter, geometric shape, and direction of pores depend on surface orientation, doping level aaaaaype, temperature, the composition of the etching conditions and applied current density.[2,3] DBR PSi has been also prepared by an applying a square current waveform to the etch cell which results two distinct indices and exhibits photonic structure of Bragg filters. In addition, chemical modification of porous silicon exhibits the modification of its physical, chemical, and electronic properties. Chemical or bio molecule can be detected by using a functionalized porous silicon.[4,5] The rugate filters were recently demonstrated to be successfully applied for the detection of different biochemical species.[6-8]

Sensitive label-free biosensors are highly desired for application in high throughput drug discovery and disease diagnostics.[9,10] Porous silicon has been employed as a large surface area matrix for immobilization of a variety of biomolecules including enzymes[11], DNA fragments[12], and antibodies.[13] Moreover, Sailor recently showed that the electronic or optical properties of

단국대학교 응용물리학과 (Department of Applied Physic, Dankook University, Yongin, 448-701, Korea)

†Corresponding author: jungdaehyuk@yahoo.com
(Received : March 4, 2010, Accepted : March 20, 2010)

porous silicon can also be used as the transducer of biomolecular interaction, thus qualifying its utility in biosensor application.[14,15]

2. Experimental

2.1. Materials and Methods

Silicon wafer (silicon sense, p^{++}-type, <100> orientation, B-doped, 0.8 ~ 0.12 mΩ) were purchased from Siltron Inc. Aquous HF (49%) and absolute ethanol (95%) were brought from Scientific Fisher. Prior to etching procedure, the silicon wafer were rinsed throughly with ethanol and dried under a steam of nitrogen. The galvanostatic etch was carried out in a Teflon cell by using a two-electrode configuration with a Pt mesh counter electrode. A sinusoidal current density waveform varying between 100 and 250 mA/cm^2 was applied. The anodization current was supplied by a Keithley 2420 high-precision constant current source controlled by a computer to allow the formation of PSi multilayers. To prevent the photogeneration of carriers, was performed the anodization in the dark. After etching, the samples are rinsed with pure ethanol and dried with nitrogen gas.

2.2. Thermal Oxidation of DBR PSi

The silicon surface was predominant hydride-terminated after the etching procedure. This surface was sensitive to oxidation and hydrolysis upon exposure to aqueous solution. Thermally oxidized porous silicon samples were obtained by heat treatment in a furnace(Thermolyne F6270-26 furnace equipped with controller)using the following parameters : intial ramp rate, 5ºC/min to 300ºC; hold time, 5hrs; and passive cooling to ambient temperature.

2.3. Functionalization of Oxidized DBR PSi

The Oxidized porous silicon sample were functionalized by refluxing them in a 50 mM solution of (3-aminopropyl)trimethoxysilane for 20 hrs. After functionalization, The sample were rinsed successively with toluene, acetone, and ethanol and subsequently dried under a stream of nitrogen. The 100 mg of Biotin (Sigma Aldrich) was dissolved in a methylene chloride solution (100 mL). the solution was stirred vigorously for 30 min, and 1-(3-(Dimethyl-amino)propyl)-3- ethylcarbodiimide hydro-chloride(EDC) (200 mg, 1 mmol) was added to the solution. The reaction mixture was allowed to stir at room temperature for 1hr. The resulting solution was added to functionalized porous silicon chip, and sample was incubated overnight. Afterward, the chip was ultra-sonicated for 3 min, and was washed 3 times with toluene, methylene chloride, and phosphate-buffered solution (PBS, pH=7.4), respectively, and dried the atmosphere.

2.4. Instrumentation and Data Acquisition

Interferometric reflectance spectra of porous silicon were recorded by using an Ocean Optics S2000 spectrometer fitted with a bifurcated fiber optic probe. A tungsten light source was focused onto the center of a porous silicon surface with a spot size of approximately 1-2 mm. Spectra were recorded with a CCD detector in the wavelength rang 400-1200 nm. The illumination of the surface as well as the detection of the reflected light was performed along an axis coincident with the surface normal.

3. Results and Discussions

3.1. Fabrication and Characterization of DBR PSi Chip

The porous shape, pore size, and orientation of porous silicon layers depend on surface orientation and the dopant level of the crystalline silicon substrate, the current density, the temperature, and the composition of the HF etching solution. Recently Hérino reported the fabrication of macropores with diameters in the range 2.5-100 nm by anodizing heavily dopped p-type silicon with a resistivity of 10^{-3} Ωcm in 25% ethanolic HF solution. Rieger and Kohl have also shown that etching p-type silicon in dry solvent such as acetonitrile or DMF in moisture-free environment results in the formation of macropore of 100 nm in p-type silicon layer. P-type silicon with resistivities of 0.1~10 Ωcm etched in ethanolic HF solution generally displays a network of micropores (diameter < 2 nm), rather than the desired well-defined cylindrical mesopores(d=2-50 nm) or macropores (d > 50 nm). Generally, the pore size of p-type 5-100 nm can be obtained by increasing the concentration of the dopant and decreasing the aqueous HF concentration, but low current densities result in random orientation of highly interconnected filament-like micropores. Large and cylindrically shape pores can be obtained when higher current densities are applied near

the electropolishing region.

3.2. Interferometric reflectance spectra

DBR PSi exhibits a high reflectivity band with a Bragg wavelength $\lambda_{Bragg,}$ depending on the thickness of the layers (d_1, d_2), and the corresponding refractive indices (n_1, n_2) The m^{th} order of the Bragg peak is given by

$$m\lambda_{Bragg} = 2(d_1n_1 + d_2n_2) \quad (1)$$

Typical etch parameters for the DBR structure involve using a periodic square wave current between low and high current densities. The dissolution times for a λ/4 layer of Bragg structures are typically from 250 s to 100 s. Its reflection band has a narrow full width at half maximum (FWHM) of 25 nm at 610 nm. DBR PSi with a reflection peak was obtained and shown in Fig. 1.

Surface and cross-sectional SEM images of PSi samples were obtained by using a cold field emission scanning electron microscope (FE-SEM, S-4800, Hitachi). FE-SEM images of DBR PSi displaying single reflection peak is shown in Fig. 2. The cross-sectional images of DBR PSi illustrates that the DBR PSi has a depth of about 11 microns. A repeating etching process results in two distinct refractive indices.

3.3. Characterization of the Functionalized porous silicon layer

Diffuse reflectance FT-IR spectroscopy was used to monitor the oxidation and functionalization reaction of the porous silicon support. The FT-IR spectrum of the porous silicon layer immediately after anodization of the porous silicon wafer displays a characteristic broad band centered at 2118 cm^{-1}. Thermal oxidation of the porous silicon layer results in the appearance of the characteristic large and broad Si-O-Si vibrational band around 1110 cm^{-1} in the FT-IR. Thermal oxidation leads to complete disappearance of the Si-H vibrational band. After functionalization of the surface with (3-aminopropyl)-trimethoxysilane, the FT-IR spectrum displays additional bands characteristic of the linker and the urea carbonyl stretching vibration of the biotin head group.

3.4. Protein A Binding to Biotinylated porous silicon surface

Fig. 3 showed the change of reflectivity in the reflection spectrum depending on the surface modification of DBR PSi. Fresh DBR PSi displayed a very sharp

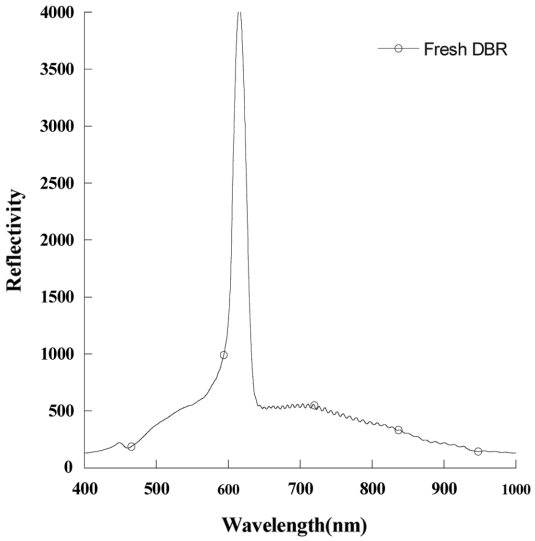

Fig. 1. Reflectivity spectrum of DBR PSi.

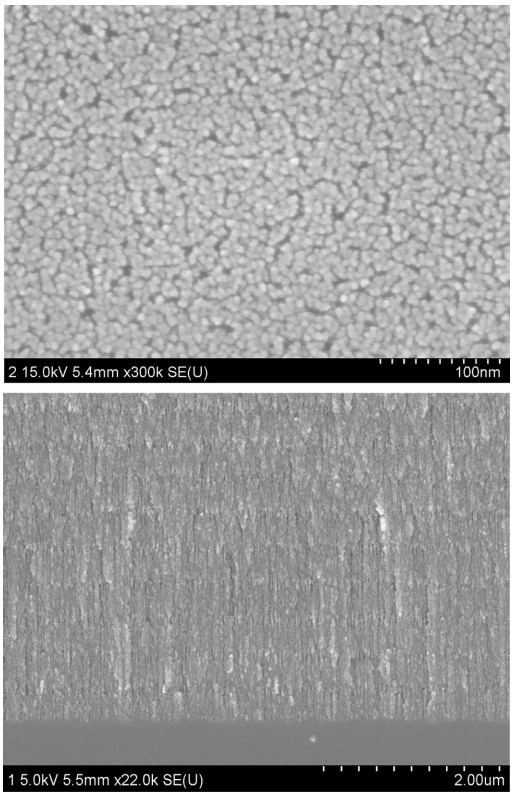

Fig. 2. Surface and cross-sectional SEM images of DBR PSi.

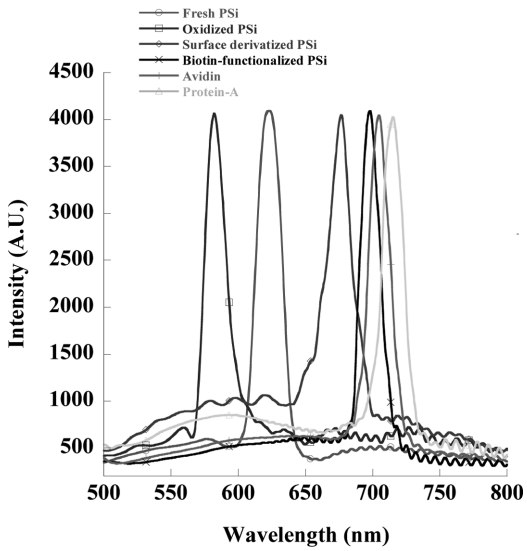

Fig. 3. Reflectivity spectra of oxidized PSi, surface derivatization and binding biomolcules DBR PSi.

reflectance resonance at 620 nm with sidelobes around the reflectance peak in the optical reflectivity spectrum. The spectral bands of DBR PSi had a full-width at half maximum (FWHM) of about 20 nm. Oxidized DBR PSi displayed a reflection resonance at 580 nm in the optical reflectivity spectrum, due to the decrease of refractive indices of the porous layer. The amine-functionalized DBR PSi resulted in the reflection resonance at 670 nm shifted to longer wavelengths, due to the increase of refractive indices upon introduction of the amine group into the pores of DBR PSi. The subsequent introduction of biotin derivatives to the amine-functionalized DBR PSi resulted in the reflection resonance at 690 nm shifted to longer wavelengths, due to the increase of additional refractive indices. For binding studies, the exposure of 20 M avidin to the biotin-functionalized DBR PSi resulted in the reflection resonance at 700 nm in the reflectivity spectrum, indicative of a change in refractive indices induced by binding of the avidin into the biotin-derivatized DBR PSi. The subsequent introduction of 20 M biotinylated protein A resulted the reflection resonance at 715 nm the reflectivity shifted to longer wavelengths by about 15 nm, indicative of a change in refractive indices induced by binding of avidin and biotinylated protein A.

4. Conclusions

The functionalized PSi biosensor was prepared for the application as a label-free biosensor based on PSi interferometer. Prepared DBR structure PSi displayed in the optical reflective spectra. The mean of construction of molecular architecture on PSi surfaces was investigated for the binding interaction with streptavidin, biotinylated protein-A. The red-shift resulted from a change in average reflective indices attributed to the replacement of some of the aqueous phases with protein.

References

[1] P. C. Canham, “Role of Si-H and Si-H2 in the photoluminescence of porous Si”, *Appl. Phys. Lett*, vol. 62, pp. 1099-1101, 1993.

[2] R. L. Smith and S. D. Collins, “Induction of articular cartilage degradation by recombinant interleukin 1 alpha and 1 beta.”, *J. Appl. Phys*. vol. 71, pp. 307-316, 1992.

[3] P. C. Searson, Advances in Electrochemical Sciences and Engineering, VCH: Mannheim, Germany, vol. 69, 1994.

[4] D. H. Yun, M. J. Song, S. I. Hong, M. S. Kang and N. K. Min, “Highly sensitive and renewable amperometric urea sensor based on self-assembled monolayer using porous silicon substrate”, *J. Korean Phys. Soc.,* vol. 47, pp. S445-S449, 2005.

[5] U. Gangopadhyay, C. Pramanik, H. Saha, K. Kim, and J. Yi, “Porous silicon as pressure sensing material”, *J. Korean Phys. Soc*. vol. 47, pp. S450-S453, 2005.

[6] Y. Y. Li, F. Cunin, J. T.Link, T. Gao, R. E. Betts, S. H. Reiver, V. Chin, S. N. Bhatia and M. J. Sailor, “Polymer replicas of photonic porous silicon for sensing and drug delivery applications”, Science vol. 199, pp. 2045-2047, 2003.

[7] T. A. Schmedake, F. Cunin, J. R. Link and M. J. Sailor, “Standoff detection of chemicals using porous silicon smart dust particles”, *Adv. Mater.*, vol. 14, pp. 1270-1272, 2002.

[8] S. O. Meade, M. S. Yoon, K. H. Ahn and M. J. Sailor, “Porous silicon photonic crystals as encoded microcarriers” *Adv. Mater.* vol. 16, pp. 1811-1814, 2004.

[9] A. Brecht and G. Sens. Gauglitz, *Actuators B.* vol. 38, no. 1, 1997.

[10] J. Janata, M. Josowicz and D. M. Devaney, “Chemical Sensors”, *Anal. Chem.* vol. 70, pp. 179R-208R,

1998.

[11] J. Drott, K. Lindstrom, L. Rosengren, T. Laurell, "Porous silicon as the carrier matrix in microstructured enzyme reactors yielding high enzyme activities", *J. Micromech. Microeng.* vol. 7, pp. 14-23, 1997.

[12] K. L. Beattie, W. G. Beattie, L. Mengm, S. L. Turner, R. Coral-Vazquez, D. D. Sith, P. M. Mcln-tyre and D. D. Dao, "Advances in genosensor research", *Clin. Chem.* vol. 41, 700-706, 1995,.

[13] T. Laurell, J. Drott, L. Rosengern and K. Lindstrom, "Enhanced enzyme activity in silicon integrated enzyme reactors utilizing porous silicon as the coupling matrix", *Sens. Actuators, B* vol. 31, pp. 161-166, 1996.

[14] V. S.-Y. Lin, K. Motesharei, K.-P. S. Dancil, M. J. Sailor and M. R. Ghadiri, "A porous silicon-based optical interferometric biosensor", *Science* vol. 278. pp. 840-843, 1997.

[15] Sailor, M. J. "Properties of porous silicon" *Data review Ser.* Canham London, no. 18, pp. 364, 1997.